*Human Molecular Genetics, 2014, Vol. 23, No. 13* **3421–3431**
*doi:10.1093/hmg/ddu051*
*Advance Access published on March 7, 2014*

# *STAG3* is a strong candidate gene for male infertility

**Elena Llano[1,*,†], Laura Gomez-H[3,†], Ignacio García-Tuñón[3], Manuel Sánchez-Martín[2], Sandrine Caburet[4,5], Jose Luis Barbero[6], John C. Schimenti[7], Reiner A. Veitia[4,5] and Alberto M. Pendas[3,*]**

[1]Departamento de Fisiología y Farmacología and [2]Departamento de Medicina, Universidad de Salamanca, 37007 Salamanca, Spain, [3]Instituto de Biología Molecular y Celular del Cáncer (CSIC-USAL), 37007 Salamanca, Spain, [4]Institut Jacques Monod, Université Paris Diderot, CNRS UMR7592, Paris 75013, France, [5]Université Paris Diderot-Paris 7, 75205 Paris Cedex 13, France, [6]Centro de Investigaciones Biológicas (CSIC), Madrid 28040, Spain and [7]Center for Vertebrate Genomics, Cornell University, Ithaca, NY 14850, USA

Received December 20, 2013; Revised and Accepted January 31, 2014

**Oligo- and azoospermia are severe forms of male infertility. However, known genetic factors account only for a small fraction of the cases. Recently, whole-exome sequencing in a large consanguineous family with inherited premature ovarian failure (POF) identified a homozygous frameshift mutation in the *STAG3* gene leading to a premature stop codon. *STAG3* encodes a meiosis-specific subunit of the cohesin complex, a large proteinaceous ring with DNA-entrapping ability that ensures sister chromatid cohesion and enables correct synapsis and segregation of homologous chromosomes during meiosis. The pathogenicity of the STAG3 mutations was functionally validated with a loss-of-function mouse model for STAG3 in oogenesis. However, and since none of the male members of this family was homozygous for the mutant allele, we only could hypothesized its putative involvement in male infertility. In this report, we show that male mice devoid of *Stag3* display a severe meiotic phenotype that includes a meiotic arrest at zygonema-like shortening of their chromosome axial elements/lateral elements, partial loss of centromeric cohesion at early prophase and maintenance of the ability to initiate but not complete RAD51- and DMC1-mediated double-strand break repair, demonstrating that STAG3 is a crucial cohesin subunit in mammalian gametogenesis and supporting our proposal that STAG3 is a strong candidate gene for human male infertility.**

## INTRODUCTION

Infertility refers to failure of a couple to conceive and affects ∼10–15% of couples (1). Among infertile couples, ∼50% are related to male infertility (2,3). Spermatogenic failure, clinically characterized by a partial or complete absence of sperm in the ejaculate, accounts for 10–15% of male infertility (4) and is divided into obstructive and non-obstructive oligo-/azoospermia. The former is characterized by a physical obstruction of the genital tract that impedes sperm from reaching the ejaculate and can be treated by testicular sperm extraction and intracytoplasmic sperm injection. In contrast, the latter is characterized by the inability to produce mature sperm and leads to severe forms of male infertility [accounting for 60% of azoospermia cases (1)]. Because of the spermatogenic failure in most non-obstructive azoospermia cases, patients are more difficult to treat (5). The non-genetic etiology of non-obstructive oligo-/azoospermia comprises heat exposure, infections, chemotherapy and radiation. The most common genetic alterations that cause non-obstructive oligo-/azoospermia include Y chromosome microdeletions and chromosomal abnormalities (6,7). However, these genetic factors only account for a reduced fraction of the cases, while in most of the patients the disease remains idiopathic (8). Determining the genetic basis of non-obstructive oligo-/azoospermia by linkage analysis is challenging because of the genetic heterogeneity and the reduced size of the families due to the intrinsic infertility. Recently, genome-wide association studies have identified several risk loci although further replication and investigations are required to evaluate their relevance and to determine the functional significance of the candidate variations, respectively (9–11). Thus, additional studies are needed for the identification of genetic mutations causative of idiopathic non-obstructive oligo-/azoospermia.

* To whom correspondence should be addressed at: Centro de Investigación del Cáncer Campus Miguel de Unamuno, Salamanca 37007, Spain. Tel: +34 923294809; Fax: +34 923284743; Email: amp@usal.es (A.M.P.); ellano@usal.es (E.L.).
†E.L. and L.G.H. contributed equally to this work.

We and others have postulated that meiotic genes affecting crucial processes during the meiotic prophase such as double-strand breaks (DSBs) generation and repair, chromosome synapsis and sister chromatid cohesion could account for a fraction of the cases of human infertility with unknown genetic etiology (12–14). Considering the phenotype of mutant mice for several meiotic genes as a model of mammalian infertility, it becomes obvious that human premature ovarian failure (POF) (OMIM #311360), the end point of primary ovarian insufficiency, would be the 'corresponding' female phenotype of oligo-/azoospermia (13,15,16).

Recently, by combining linkage data and exome sequencing in a consanguineous POF family, we have identified a homozygous 1-base pair (bp) deletion in the *STAG3* gene, leading to a truncated coding sequence in four sisters affected with POF, whereas their unaffected parents were heterozygous carriers (17,18). The fertile siblings (both males and females) were either heterozygous or homozygous for the wild-type allele. *STAG3* is a meiosis-specific component of the cohesin complex, a large ring-shaped proteinaceous structure that tethers sister chromatids (i.e. cohesion) (19). The somatic cohesin complex is composed of four main subunits, Smc1α, Smc3, Rad21 and the stromal antigen proteins STAG1 or STAG2. SMC1α and SMC3 belong to the structural maintenance of chromosome family. SMC proteins have one adenosine triphosphate (ATP)-binding cassette-like domain with ATPase activity formed by the interaction of the N- and C-terminal domains. These domains are joined by the autofolding of the protein by the so-called hinge region forming long antiparallel coiled coils. In addition, the hinge region is the interacting domain that mediates dimerization of both SMCs. Together, they form a V-shaped Smc1α/Smc3 heterodimer which is closed by the tight interaction of RAD21 with the ATPase heads of Smc1α and SMC3 via its N- and C-terminus, resulting in a closed ring-shaped structure (20). Finally, the STAG subunit associates to the complex by binding to the C-terminal region of the Rad21 α-kleisin subunit. In addition, there are meiotic-specific paralogues of Rad21, STAG1/2 and SMC1α, respectively RAD21L and REC8, STAG3 and SMC1β (21–23). By its ability to foster DNA looping, the cohesin complex also participates in DSBs processing and synapsis of homologous chromosomes during the prophase I of meiosis (24). These functions rely on the essential role that cohesins play in the assembly of the synaptonemal complex (SC), a tripartite proteinaceous scaffold that forms between the paired homologous chromosomes (25).

In relation to the mutation in the *STAG3* gene affecting the POF family, we validated its pathogenicity by describing a loss-of-function mouse model for *Stag3*. Mutant mice lacking STAG3 showed no overt somatic phenotype but deficient female mice were sterile and displayed a premature meiotic arrest with degenerating ovaries, which were devoid of follicles by 1 week of age.

Despite the informativity of the aforementioned POF family, none of the male individuals was homozygous for the mutant allele. Here, we analyze the mutant phenotype of male mice deficient for *Stag3*. We demonstrate that the STAG3-deficient males display a severe defect in synapsis and premature loss of centromeric cohesion at early stages of prophase I which provokes an arrest at zygotene-like stage and leads to infertility. This model clearly shows that *STAG3* is a very strong candidate gene of non-obstructive oligo-/azoospermia in humans.

## RESULTS AND DISCUSSION

We have previously shown that the female mouse line OVE2312C, generated by a lentiposon insertional mutation in the intron 8 of *Stag3* harbours a null allele that leads to a depletion of the *Stag3* transcript and its corresponding encoded STAG3 protein (18). *Stag3*-deficient female mice showed no overt somatic phenotype apart from the lack of oocytes and ovarian follicles at 1 week of age and the presence in their ovaries of a dense stroma, indicating a severe ovarian dysgenesis. Oocytes from female null embryos (from 15.5 to 19.5 dpc) showed a very early meiotic arrest (leptotene like) with complete absence of synapsis (18).

Since the phenotype of meiotic mouse mutants commonly show sexual dimorphism (13,26,27), we analyzed spermatogenesis to validate *Stag3* as a non-obstructive oligo-/azoospermia candidate gene. Heterozygous mice displayed no phenotype and were fully fertile with normal testes and spermatogenesis (data not shown). We analyzed testes from adult (2–8 months; $n = 12$) $Stag3^{-/-}$ mice and showed that they were on average 78% smaller than those from wild-type mice, and their epididymides did not contain spermatozoa upon histological examination (Fig. 1A and B). Histological analysis revealed the absence of post-meiotic cells although spermatogonia, Sertoli and Leydig cells were apparently normal (Fig. 1B). The seminiferous epithelium from the mouse contains a mixture of germ cells at various developmental stages. Staging of each section of the tubule is defined (from I to XII) according to the set of associated germ cell types that are present (28). Following these criteria, the most advanced type of meiocytes were spermatocytes with nuclear chromatin characteristic of zygotene/pachytene-stage cells which were present in seminiferous tubules arrested at Stage IV of the epithelial cycle (Fig. 1B). This is the developmental stage at which most of the meiotic mutants are arrested (29), leading to a massive degeneration (Fig. 1B). In addition, we carried out a fluorescence-activated cell sorting (FACs) analysis of whole cells from seminiferous tubules and showed the absence of the haploid compartment in $Stag3^{-/-}$ testes, which supports the prophase I arrest (Fig. 1D). Given the lack of spermatozoa and the reduced weight of the testis, we carried out Terminal deoxynucleotidyl transferase dUTP nick end labeling (TUNEL) staining and showed that the number of apoptotic cells in $Stag3^{-/-}$ tubules was higher than in wild-type (Fig. 1C), which likely corresponds to the massive degeneration and accounts for the reduced size of the testis.

### SC assembly in Stag3-deficient spermatocytes

To functionally characterize more precisely the infertility and the meiotic arrest in the *Stag3* knockout (KO) mice, we also analyzed meiocytes from male seminiferous tubules by immunofluorescent staining of the Synaptonemal Complex Protein 3 (SYCP3) component of the axial element (AE) of the SC and the transverse filament protein SYCP1, a marker of synapsis, on chromosome spreads. Wild-type meiocytes start to build their AEs at leptotene (short threads) and start to synapse at zygotene (large threads) until they are fully synapsed at the pachytene stage which is characterized by 19 pairs of full-length synapsed homologs (autosomes) and a partially synapsed sex bivalent at the pseudoautosomal region (Fig. 2). However, in the

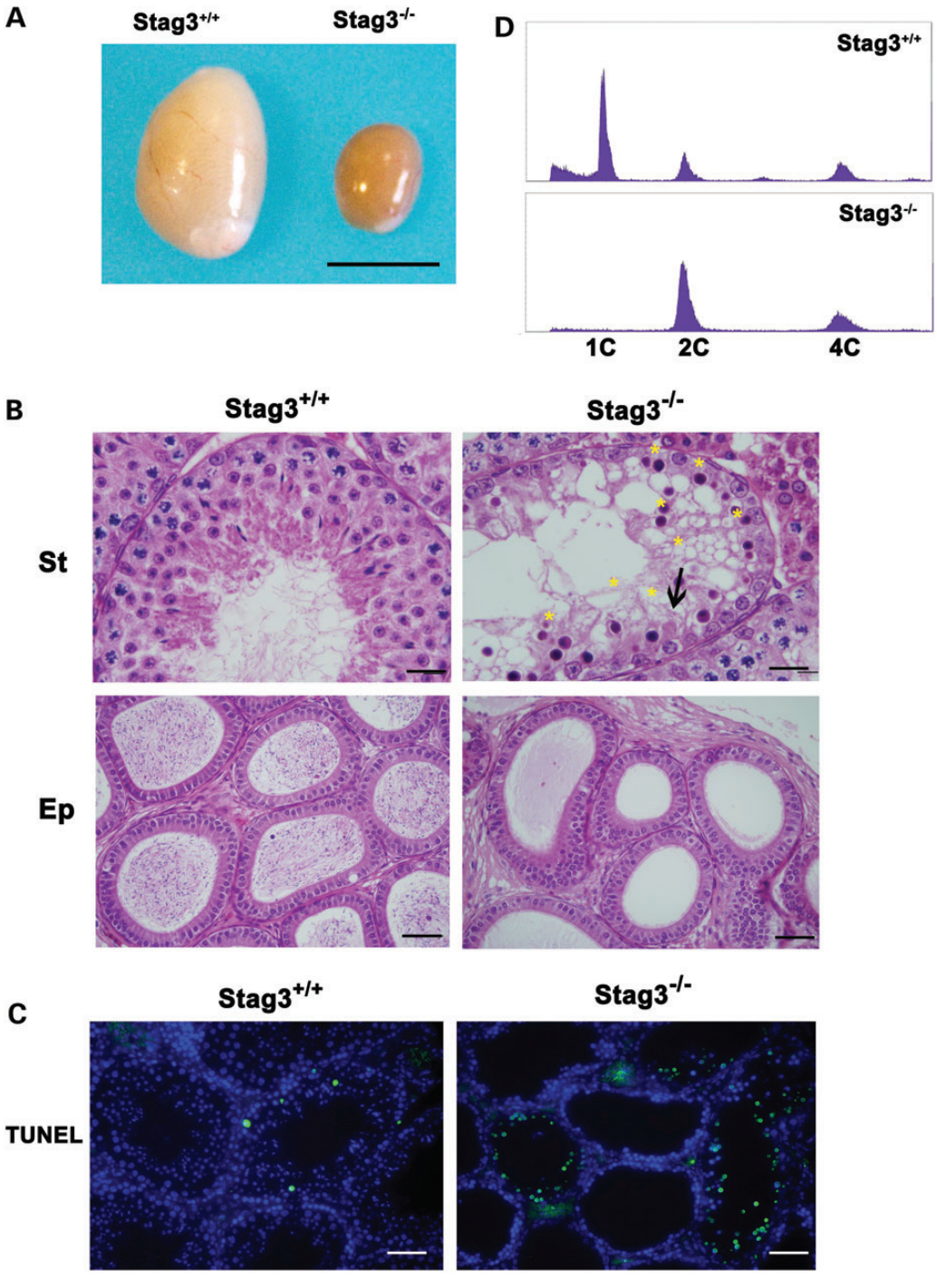


**Figure 1.** Mice lacking STAG3 are azoospermic. (**A**) Genetic ablation of *Stag3* leads to a reduction in testis size. (**B**) *Stag3*$^{-/-}$ seminiferous tubules arrested at Stage IV of the epithelial cycle are characterized by intermediate spermatogonia (arrows) ready to divide into type B spermatogonia. Massive degeneration of spermatocytes (asterisks) can be seen. The complete block of the spermatogenesis leads to empty epididymides and non-obstructive oligo-/azoospermia. (**St**) Seminiferous tubules. (**Ep**) Epididymides. (**C**) Immunofluorescence detection apoptotic cells by Terminal deoxynucleotidyl transferase dUTP nick end labeling (TUNEL) staining show an increase of apoptotic cells in *Stag3*$^{-/-}$ seminiferous tubules. (**D**) Abnormal ploidy of *Stag3*$^{-/-}$ spermatocytes. FACs analysis of cells from seminiferous tubules showing the absence of the haploid compartment in *Stag3*$^{-/-}$ testes. Bar in panel A is 5 mm. Bar in upper panel B is 20 μm and 75 μm in lower panel B (Ep) and C (TUNEL).

absence of STAG3, AE assembly and synapsis between homologs were disrupted very early (Fig. 2). *Stag3*$^{-/-}$ spermatocytes were apparently arrested at a zygotene-like stage and never reached pachytene (100%) but with differentiated types of arrest that were grossly classified for the analysis in two extreme classes. The most frequent arrested meiocytes (65% L-type spermatocytes; $n = 100$) were characterized by the presence of thin and discontinuous SYCP3 threads corresponding to

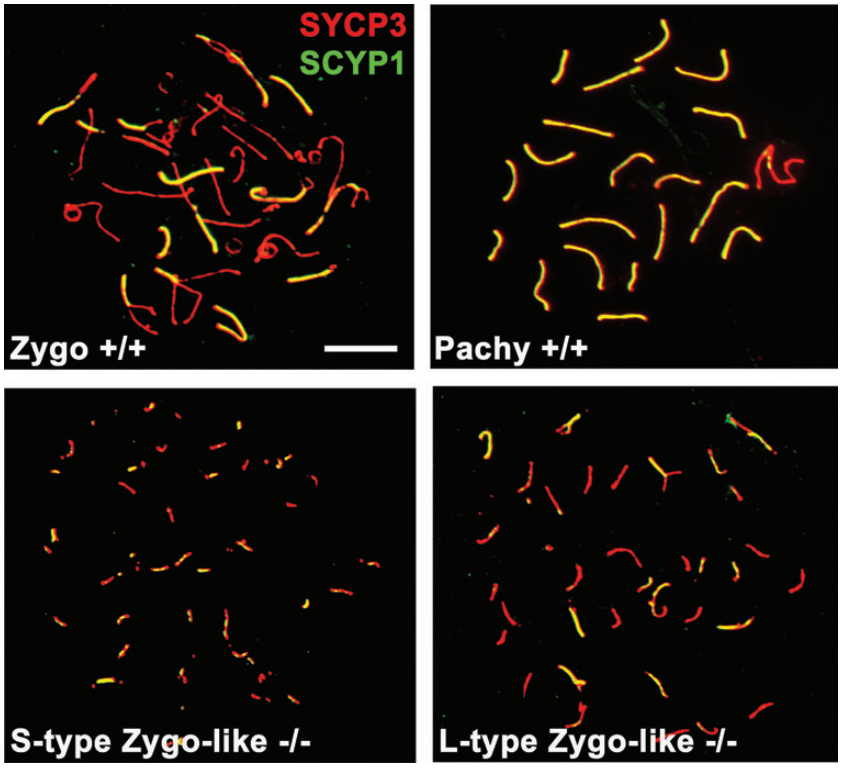


**Figure 2.** *Stag3*$^{-/-}$ spermatocytes show defects in synapsis. Double labeling of Synaptonemal Complex Protein 3 (SYCP3) (red) and SYCP1 (green) showing fragmented (right; type-L-arrested spermatocytes) or shortened (left; type-S-arrested spermatocytes) AEs/LEs with partial synapsis and with patches of SYCP1 in mutant spermatocytes compared with their wild-type control. Bar represents 2.5 μm.

the AEs and some partially synapsed lateral elements (LEs; positive staining for SYCP1) that never progressed to the expected 19 fully synapsed autosomal bivalent chromosomes observed in wild-type pachynema (Fig. 2). On the other hand, the less frequent *Stag3*$^{-/-}$-arrested meiocytes (35% $n = 100$; S-type spermatocytes) showed very short AEs that although apparently desynapsed as independent very short AEs (~40), they showed partial SYCP1 labeling (Fig. 2). These arrested meiocytes showed a very severe meiotic phenotype (although partially resembling previous single meiotic mutants). Thus far, only *Rec8*$^{-/-}$*;Rad21L*$^{-/-}$ double knockout spermatocytes show a more severe phenotype in AE assembly and pairing (12) than *Stag3*$^{-/-}$ spermatocytes. Rec8 and Rad21L have been shown to interact exclusively with STAG3 cohesin complexes but not with STAG1 or STAG2 (30). Therefore, the defect on AE assembly in *Stag3*$^{-/-}$ and *Rec8*$^{-/-}$*;Rad21L*$^{-/-}$ spermatocytes are expected to be similar. The differences observed here suggest that in the absence of STAG3, another molecule might form functional complexes with Rec8 and Rad21L. STAG1 and/or STAG2 might be candidates but they have not been functionally implicated thus far in AE assembly. To further analyze this possibility, we immunolabeled STAG1 and STAG2 in STAG3-deficient spermatocytes and show no evidence of a compensatory mechanisms involving these molecules (i.e. such us upregulation of their expression, Supplementary Material, Fig. S1).

To further quantitatively analyze the synaptic defects, we studied the centromere distribution by immunofluorescence with a human anti-centromere antibody (ACA) (Fig. 3) in both types of *Stag3*$^{-/-}$-arrested meiocytes. In wild-type spermatocytes at leptotene, the number of centromere foci never exceeded 40. As synapsis progressed, these centromeric foci merged into 21 signals (19 signals from synapsed autosomes + 2 signals for the XY bivalent) at pachytene when homologous synapsis is complete and their centromeres are closely juxtaposed. In *Stag3*$^{-/-}$ zygotene-like L-type spermatocytes we scored on average 42.47 ± 1.28 foci ($n = 30$ nuclei), whereas in zygotene-like type S spermatocytes we scored on average 46.55 ± 2.7 ($n = 30$). This result suggests the existence of a virtual lack of synapsis between homologs, at least at their centromeric regions (Fig. 3) but, more interestingly, a partial lack of centromeric cohesion. To evaluate this in more detail, we quantified the number of chromosomes presenting two close ACA signals per chromosome (2.35 ± 1.25 for L-type and 6.18 ± 2.69 for S-type Stag3$^{-/-}$ spermatocytes; $n = 31$) in comparison with the wild-type in which all of the cells show a single signal per chromosome (Fig. 3). This observation is congruent with the fundamental role that the somatic cohesin complex plays in sister chromatid cohesion. To evaluate whether this function is also carried out by the Rec8-containing cohesin complex, which is considered to be the canonical meiotic cohesin involved in the cohesion of dyads and chromatids (31,32), we analyzed arrested spermatocytes lacking REC8, which did not show such a loss of sister chromatid cohesion at the centromeres (for comparison, see Supplementary Material, Table SI) However, as expected although not previously demonstrated, we observed loss of sister chromatid cohesion at the centromeres of okadaic

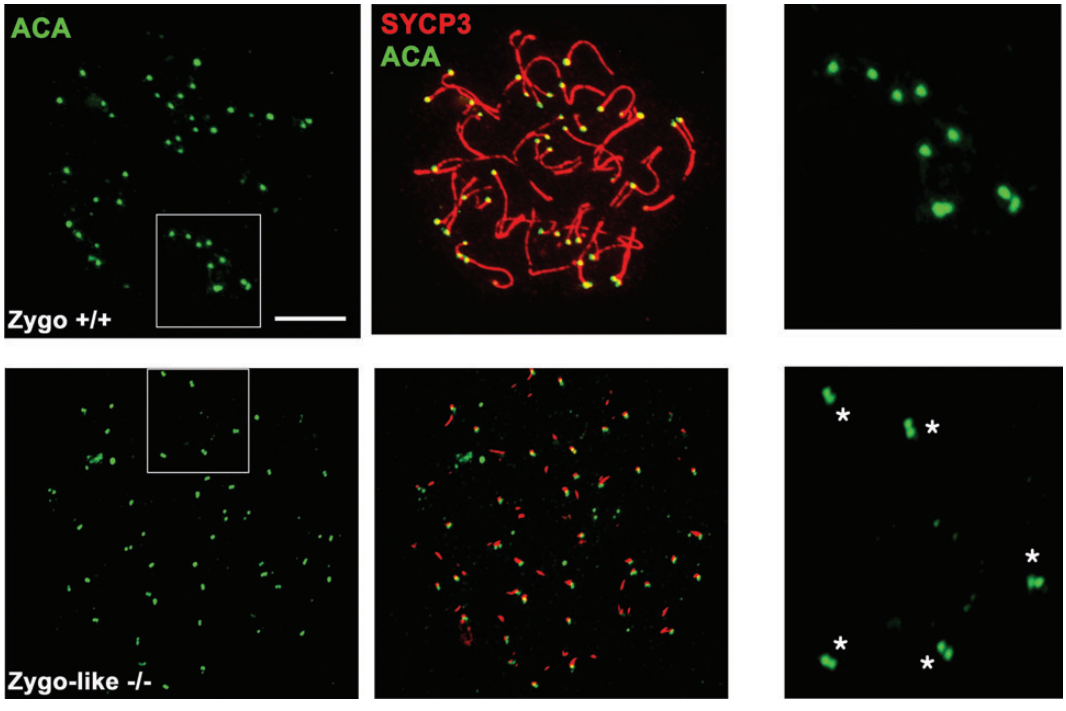


**Figure 3.** STAG3 deficiency leads to premature loss of cohesion. Double immunofluorescence of SYCP3 (red) and ACA (green). Wild-type zygotene spermatocytes show 40 single signals of ACA at one end of the AE/LEs. However, the number of ACA signals exceeded 40 in *Stag3*$^{-/-}$ zygotene-like arrested spermatocytes because of the presence of chromosomes with two close but not juxtaposed ACA signals (asterisks depicted in the left lower magnified panel). In the wild-type, the spermatocytes displayed a single signal per chromosome (left upper magnified panel). Bar represents 2.5 μm.

acid (OA)-induced *Rec8*$^{-/-}$ spermatocytes (Supplementary Material, Fig. S2). As a control of spermatocytes with unjoined chromosomes at metaphase I but without loss of centromeric cohesion, we used OA-induced spermatocytes from RAD21L-deficient spermatocytes and showed the expected 40 univalents with joined chromatids (13; Supplementary Material, Fig. S2).

This lack of cohesion was also observed in the chromosomes from oocytes lacking STAG3 although with a higher penetrance (18). Mutations in mice that affect other meiotic cohesin subunits also result in abnormal spermatocyte development with meiotic arrest at zygotene/pachytene-like stage because of abnormal AE formation/synapsis. However, their meiocytes were not reported to show any lack of centromeric cohesion at zygonema [REC8, this work; SMC1β (15) and RAD21L this work and (13)]. Inrestingy, a very recent re-analysis of SMC1β-deficient spermatocytes in a null SPO11 background showed loss of centromeric sister chromatid cohesion in the 35% of the AEs when homolog association was disrupted (33). We can speculate that the lower penetrance of the loss of centromeric cohesion in the REC8-deficient mice, in comparison with the STAG3 mutants, could be due to the existence of partial synapsis between homologs which mask the doublets ACA foci as single ACA signals in the absence of centromeric cohesion. Further, analysis of the REC8 mutants in a null SPO11 background (no DSBs are generated) would partially unravel this point. Taken together, these results suggest that the cohesion function at the centromeres is carried out by a cohesin complex containing STAG3, SMC1β and REC8.

In summary, these results indicate that STAG3 is an important meiotic cohesin subunit, since STAG3-containing cohesin complexes are essential for chromosome synapsis and maintenance of centromeric sister chromatid cohesion in the early stages of prophase I.

### DSBs generation and defective repair occurs in Stag3$^{-/-}$-arrested spermatocytes with shortened AEs

To elucidate the cause of the meiotic arrest, we analyzed meiotic chromosomes with a variety of markers that are diagnostic of recombination. First, we analyzed the SPO11-promoted DSBs at the leptotene stage by immunolabeling of phosphorylated histone variant γ-H2AX (34). This phosphorylation occurs during early prophase I in response to SPO11-induced DSBs in an ATM-dependent manner and disappears from the autosomes towards pachytene as the DSBs get repaired (35). All the Stag3$^{-/-}$ spermatocytes showed a positive γ-H2AX staining at leptotene ($102.6 \pm 41.6$ versus $94.8 \pm 27.9$; $n = 35$; Fig. 4A) that was partially reduced at the zygotene-like arrest in a similar fashion to the wild-type spermatocytes. This result suggests that the generation of the DSBs is not affected by the STAG3 deficiency and that the DSBs are not resolved in the arrested spermatocytes.

We subsequently addressed why DSBs are not repaired in the mutant spermatocytes. After DSBs are generated, the recombinases RAD51 and DMC1 are recruited to promote homolog searching by strand invasion (36). In wild-type leptotene spermatocytes, RAD51 and DMC1 assemble on the AEs/LEs of chromosomes and gradually disappear towards pachynema (37). As shown in Figure 4B, wild-type spermatocytes showed both RAD51 and DMC1 foci, whereas *Stag3*$^{-/-}$-arrested

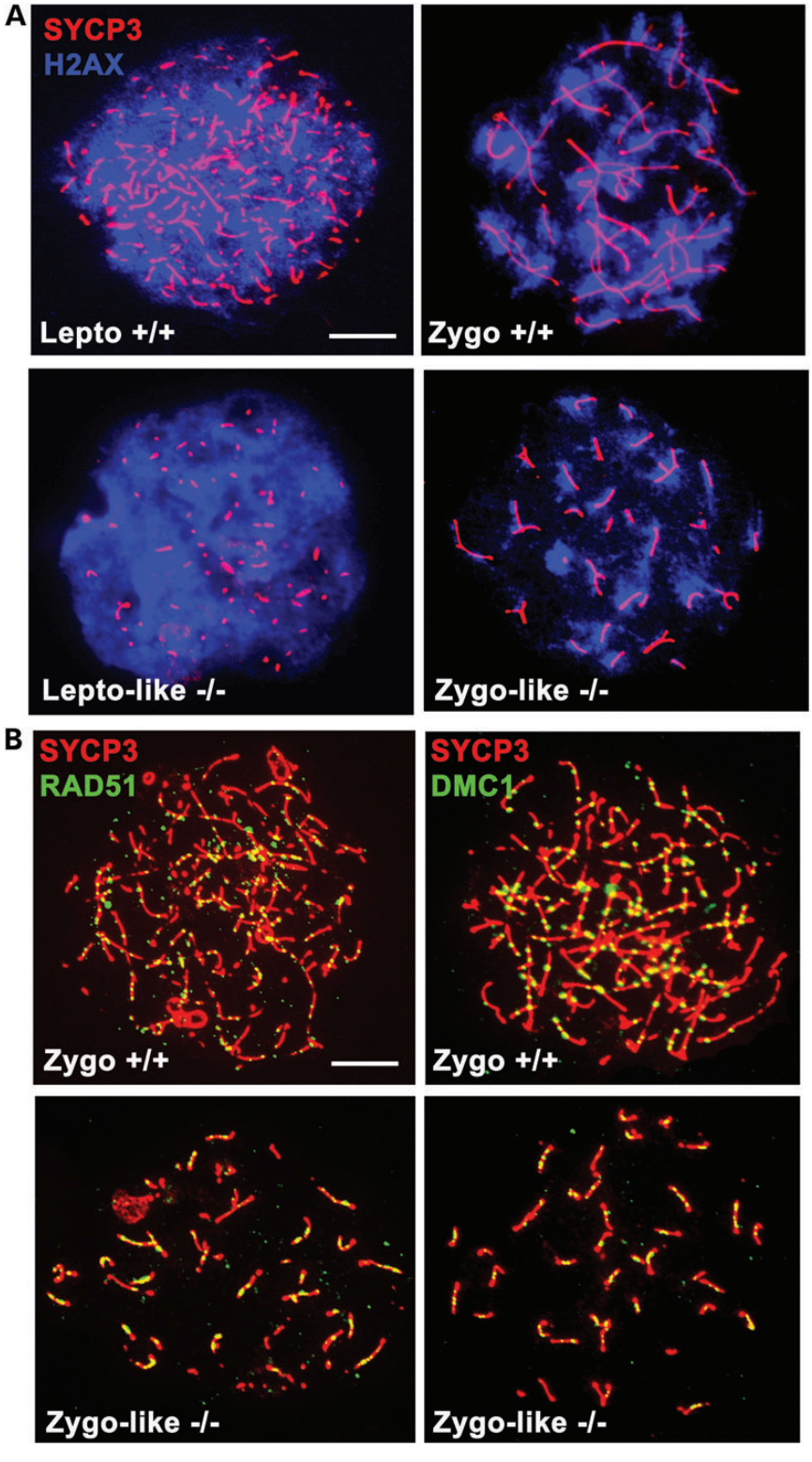


**Figure 4.** Programed DSBs are generated but defectively repair in STAG3-deficient spermatocytes. (**A**) Double immunolabeling of SYCP3 (red) with γH2AX (blue) in *Stag3*$^{+/+}$ and *Stag3*$^{-/-}$ spermatocytes. In wild-type spermatocytes at leptonema, γH2AX labels intensely the chromatin of the spermatocytes. At zygonema, the labeling is partially reduced until pachynema when the signal disappears, remaining only at the chromatin of the unsynapsed sex bivalent (data not shown). Similarly, in the STAG3 KO, γH2AX also labels the chromatin at leptotene stage and more faintly at zygonema, where it remains during the whole meiotic arrest, suggesting that DSBs are partially but not completely repaired. **(B)** Double immunolabeling of SYCP3 (red) and RAD51 or DMC1 (green) in wild-type and *Stag3*$^{-/-}$ spermatocytes. In both wild-type spermatocytes and *Stag3* mutants, RAD51 and DMC1 localize to AE/LEs at zygonema; however, the number of foci is reduced 2-fold. Bar represents 2.5 μm.

**Table 1.** Quantification of RAD51 and DMC1 foci

| | Number of RAD51 foci | Number of DMC1 foci |
|---|---|---|
| Wild-type | 132.6 ± 20.1; $n = 22$ | 155.6 ± 39.2; $n = 20$ |
| Stag3 KO L-type | 69.7 ± 11.4[a]; $n = 22$ | 86.9 ± 15.4; $n = 22$ |
| Stag3 KO S-type | 67.5 ± 9.9[a]; $n = 22$ | 85.6 ± 11.7; $n = 22$ |

[a]Significantly different from wild-type ($P < 0.001$).

spermatocytes showed a reduction in the number of RAD51/DMC1 foci (Fig. 4B and Table 1). Thus, the loading of the RAD51/DMC1 is not impaired but significantly reduced in the absence of STAG3, and this insufficient loading together with the synapsis defects likely leads to the observed unrepaired DSBs.

To determine whether the short AEs observed in the arrested spermatocytes correspond to shortened AEs or to partial fragmented/discontinuous AEs, we immunolocalized the telomeric protein RAP1 (13,38). The results showed that most of the RAP1 foci were mapped at both ends (telomeres) of the short AEs of the arrested *Stag3*$^{-/-}$ spermatocytes, suggesting that they are indeed shortened AEs and not discontinuous or fragmented ones (Supplementary Material, Fig. S3). A similar 'shortening' phenotype has also been reported in *Smc1B*$^{-/-}$ spermatocytes (15). However, because *Smc1B*$^{-/-}$ spermatogenic blockade occurs in a later stage of the meiotic prophase (early/mid pachytene), the arrested spermatocytes showed a reduction in the length of their already partially synapsed AE/LEs instead of in the asynapsed *Stag3*$^{-/-}$ AEs. Interestingly, since *Stag3*$^{-/-}$ oocyte arrest is as early as leptotene and that AEs are still not assembled in threads, similar to the double deficiency for RAD21L and REC8 (12), the shortening of the asynapsed AEs was not observed (18). The role of STAG3-containing cohesin complexes in the length of the AEs and thus in DNA looping (15,39) might rely only on the formation of a complex with SMC1β. However, our cytological observations showing only a partial reduction of the loading of SMC1β into the *Stag3*$^{-/-}$ AEs do not fully support this hypothesis (see below). Instead, we propose that this severe shortening occurs also by additional STAG3-containing cohesin complexes (i.e. those complexed with SMC1α), given that STAG3 can complex with the two SMC1 subunits, SMC1α and SMC1β (30) which are co-expressed in the testis.

### OA-induced metaphase I chromosomes show absence of chiasma and loss of centromeric cohesion

We next sought to analyze whether crossing over (CO) and chiasmata could be formed in the absence of the meiotic arrest that prevents mutant spermatocytes to enter into pachytene, as well as in the absence of STAG3 function in centromeric cohesion at metaphase I. To do this, we cultured wild-type and KO spermatocytes in the presence of OA (a PP2A inhibitor), to allow *in vitro* transition from zygotene to metaphase I (40). OA-treated wild-type spermatocytes showed 20 bivalents joined by at least one chiasma and were positive for SYCP3 labeling at the interchromatid and centromeric domain. Bivalents always showed two pairs of unseparated sister kinetochores by ACA staining (Fig. 5). However, OA-treated *Stag3*$^{-/-}$ spermatocytes displayed 80 unattached chromatids with labeling for SYCP3 at some centromeres but also as aggregates (Fig. 5). This phenotype was similar in OA-treated *Rec8*$^{-/-}$ spermatocytes (Fig. S2). As noted above, in early prophase, Stag3$^{-/-}$ (and to a much lesser extent in *Rec8*$^{-/-}$) spermatocytes display a partial loss of centromeric cohesion. These results suggest the existence of some degree of cohesin turnover during or after prophase I or alternatively, the existence of technical limitations in the chromosome spread and/or microscopic resolution that might obscure the detection of loss of cohesion at all the centromeres. Similarly, *Smc1β*$^{-/-}$ spermatocytes show partial loss of sister chromatid cohesion at prophase I (33) and complete loss of centromeric cohesion at OA-induced metaphase I (15). Altogether, these observations firmly support that STAG3/SMC1β-containing cohesin complexes are necessary for the centromeric cohesion at metaphase I and chiasma formation, and support, but not demonstrate, that the role of these STAG3/SMC1β-containing cohesin complexes in centromeric cohesion is very likely performed through interactions with REC8, although perhaps not exclusively.

### Complexes of STAG3 with other cohesin subunits

The absence of the two meiosis-specific cohesin subunits RAD21L and REC8 prevents the normal loading of other cohesins and the assembly of AEs. Thus, we analyzed whether the loss of STAG3 also compromised the loading of other cohesins in spermatocytes. The double immunofluorescence of the various meiotic cohesin subunits and SYCP3 in wild-type and *Stag3*$^{-/-}$ spermatocytes showed that the loss of STAG3 induced a reduction in the co-localization of SMC1β with SYCP3 (Fig. 6). Thus far, the effect on the localization of other cohesin subunits has been shown to be stronger only in *Rec8*$^{-/-}$*;Rad21L*$^{-/-}$ double knockout spermatocytes (12). Interestingly, although Rec8 immunolabeling was observed, it was close to our limit of detection. Rad21, SMC3 and RAD21L immunolocalization was not apparently affected (Fig. 6). Interestingly, this phenotype was more severe in the *Stag3*$^{-/-}$ oocytes where Rec8 was not detected at all using the same procedures and antibodies (18), indicating that there is a sexual dimorphism in the different STAG3-containing cohesin complexes. Female meiosis would thus be more dependent on STAG3-containing cohesin complexes than male meiosis. This sexual dimorphism could be explained if we accept that RAD21L could have STAG3-independent functions such as those performed at the sex body and the inner centromere at metaphase I and II (13,41), two cytological domains that are exclusively labeled by RAD21L antibodies at male meiosis (i.e. no other cohesins co-localize at these sites). Further studies are needed to provide a mechanistic explanation.

Overall, these results indicate that in spermatocytes STAG3 is complexed *in vivo* with REC8 and with SMC1β, and is apparently independent of the kleisins RAD21 and RAD21L. Under a simple model of the cohesin complex in which the lack of one subunit impedes the association of the remaining subunits of the complex and their detection along the AE/LEs, these data are not congruent with the deficient loading of STAG3 in *Rad21l*$^{-/-}$ spermatocytes (13) and would resemble to some extent the RAD21L-deficient oocytes in which STAG3 labeling was not altered (13). Similarly, the genetic ablation of *Rec8* does

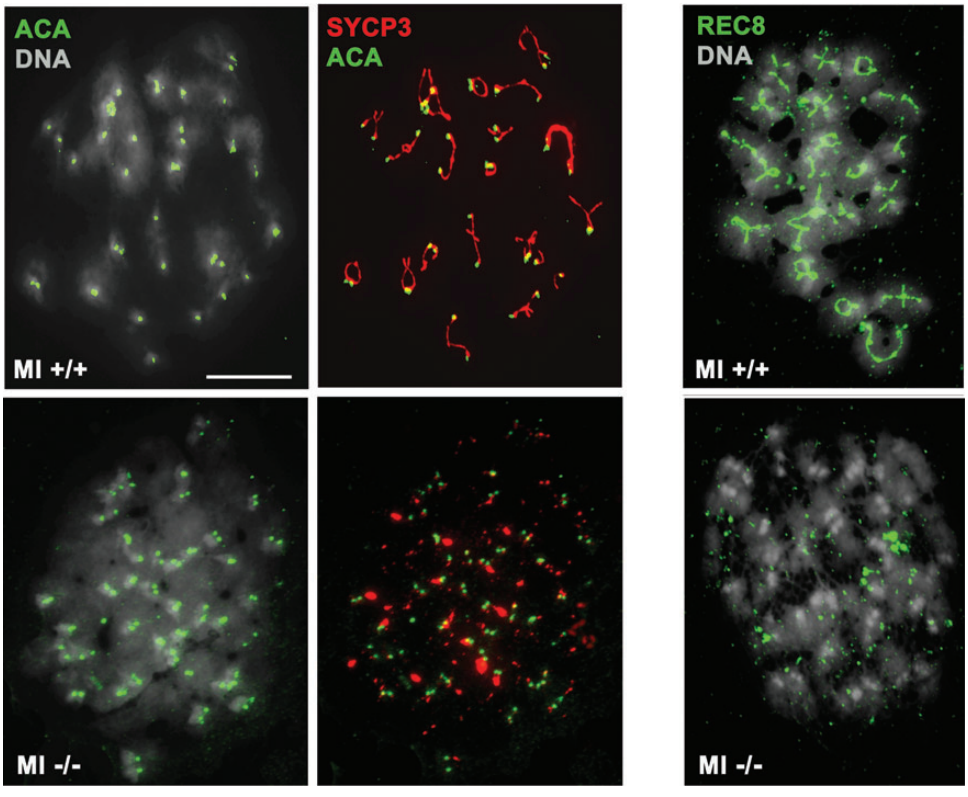


**Figure 5.** The deficiency of STAG3 prevents CO and leads to total loss of centromeric cohesion at metaphase I. Double immunolabeling of SYCP3 (red) or REC8 (green) with ACA (green) and 4',6-diamidino-2-phenylindole (blue) in wild-type and *Stag3*$^{-/-}$ spermatocytes. OA-induced metaphase I plates of wild-type spermatocytes give rise to 20 bivalents each with two opposed centromere signals (ACA) and positive for SYCP3 and REC8 labeling at the interchromatid and centromeric domain, whereas *Stag3*$^{-/-}$ spermatocytes lead to 80 separated centromere signals with ACA and delocalization of SYCP3 and REC8 labeling from the centromeres (aggregates). Bar represents 2.5 μm.

not substantially alter the immunodetection of SMC1β nor STAG3 (Supplementary Material, Fig. S4) and, in turn, SMC1β deficiency does not alter neither the loading of REC8 nor that of STAG3 (15). Thus, and although counterintuitively, it seems that the interactions between subunits are not always reciprocal. This deserves further exploration.

From a cohesive point it can be noted that (i) RAD21L-deficient meiocytes do not present defects in cohesion (13 and Supplementary Material, Fig. S2), (ii) REC8 mutants exhibit a faint loss of centromeric cohesion at prophase I that leads to a total loss of cohesion in the OA-induced metaphase I (15,16,42 and Supplementary Material, Fig. S2), (iii) STAG3 and SMC1β mutant spermatocytes show premature loss of centromeric cohesion at very early prophase (18,33, Fig. 3) and iv) STAG3 mutant oocytes, but not SMC1β, show premature loss of cohesion (15,17). This shows that STAG3 is a crucial meiotic cohesin subunit in the maintenance of centromeric cohesion in early prophase I. We propose that STAG3 (likely complexed with SMC1β and REC8) is essential for the maintenance of centromeric sister chromatid cohesion in spermatocytes starting at early prophase I until metaphase I.

STAG3 is thus essential for mammalian gametogenesis in both males and females and is arguably the most relevant single meiotic cohesin since none of Rad21l, Smc1β and Rec8 mouse mutants (13,15,16,42) shows a meiotic phenotype as severe as the one described in males (this work) and in female mice (18).

*STAG3* mutations causing a recessive form of non-obstructive oligo-/azoospermia are most likely to be at a heterozygous state in the general human population, as was the case in the fertile men carrying the *STAG3* mutation in the previously reported POF family (18). However, the existence of homozygotes and compound heterozygotes for recessive mutations or even the existence of dominant forms acting through a dominant negative mechanism, as has been demonstrated for the recombinase DMC1 in the mouse (43) and suggested in humans (44), is plausible and expected. In the latter case, a heterozygous mutation in *STAG3* would poison the macromolecular complexes in which it is involved and lead to infertility (ranging from azoospermia for the most damaging homozygous mutations to milder conditions).

In conclusion, this study identifies a crucial role of the cohesin subunit STAG3 in male spermatogenesis through the analysis of a loss-of-function mouse model. Male mice lacking STAG3 were infertile and showed a severe meiotic phenotype that included a meiotic arrest at zygonema-like with shortening of their chromosome AE/LEs and loss of centromeric cohesion. Our results indicate that STAG3-containing cohesin complexes are essential for mammalian gametogenesis and support our initial proposal that STAG3 is a strong candidate gene for human male infertility.

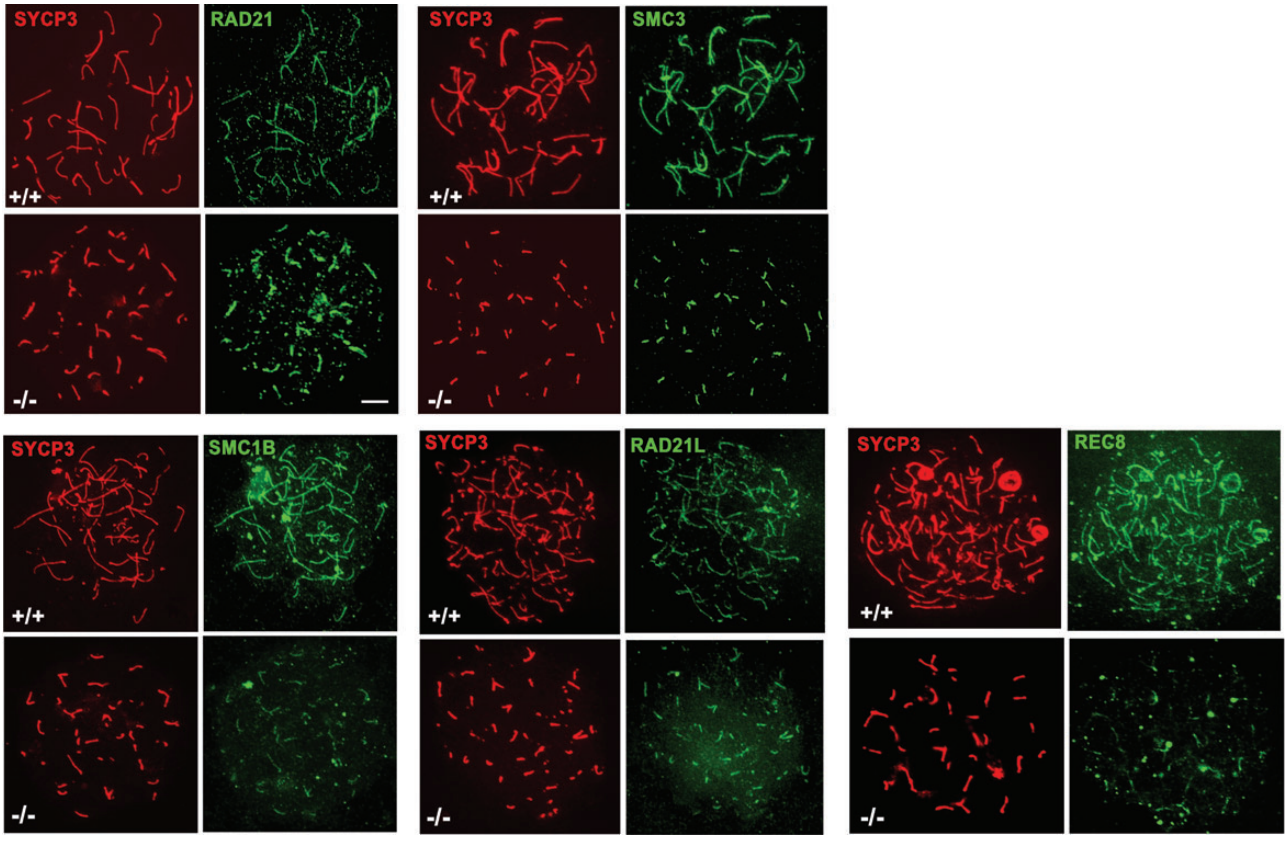


**Figure 6.** Complexes of STAG3 with other cohesin subunits. Double immunolabeling of SYCP3 (red) with RAD21, SMC3, SMC1β, RAD21L or REC8 (green) in spermatocytes. In wild-type zygotene spermatocytes, the cohesin subunits RAD21, SMC3, SMC1β, RAD21L and REC8 colocalize with SYCP3 along the AEs of the chromosomes. However, in spermatocytes from *Stag3*$^{-/-}$ arrested at a zygotene-like stage, SMC1β showed a moderate immunofluorescence reduction, whereas REC8 showed a more intense immunolabeling reduction in comparison with SYCP3. RAD21, RAD21L and SMC3 immunolabeling was not affected by the loss of STAG3. Bar represents 2.5 μm.

## MATERIALS AND METHODS

### Immunocytology and antibodies

Testes were detunicated and processed for spreading using the 'dry-down' technique (45). The primary antibodies used for immunofluorescence were rabbit αSMC3 serum K987 (1:20), rabbit αSMC1β serum K974 (1:20) (46), rabbit αSTAG3 serum K403 (1:20) (22), αREC8 serum K1019 (13), rabbit αRAD21 IgG K854 (1:5) (43), mouse αSYCP3 IgG sc-74569 (1:100), rabbit αRAD51 sc-8349 (1:30) and PC130 (1:50), rabbit αDMC1 sc-22768 (1:20) (Santa Cruz Biotechnology, CA, USA), rabbit α-STAG2 ab422 (1:20), rabbit α-STAG1 (1:20), rabbit αSYCP1 IgG ab15090 (1:200) (Abcam, Cambridge, UK), rabbit anti-γH2AX (ser139) IgG #07-164 (1:200) (Millipore, Eschborn, Germany), ACA or purified human α-centromere proteins IgG 15-235 (1:5, Antibodies Incorporated), rabbit αRAP1 IgG (1:400, provided by Dr Titia de Lange, The Rockefeller University, New York, NY, USA) and rabbit αRPA IgG (1:300, provided by Dr E. Marcon, Toronto University, Canada). The secondary antibodies used were tetramethylrhodamine isothiocyanate α-mouse 115-095-146/α-rabbit 111-025-144 and fluorescein isothiocyanate α-mouse 115-095-146/α-rabbit 111-095-045 (Jackson ImmunoResearch, West Grove, PA, USA) (all 1:100). Slides were visualized at room temperature using a microscope (Axioplan 2; Carl Zeiss, Inc., Jena, Germany) with 63 × objectives with an aperture of 1.4 (Carl Zeiss, Inc.). Images were taken with a digital camera (ORCA-ER; Hamamatsu) and processed with OPENLAB 4.0.3 and Photoshop (Adobe, Mountain View, CA, USA). Quantification of γH2AX fluorescence signal was measured by the Image J software.

### Mice

The OVE2312C mouse line was obtained from the Jackson Laboratory. It harbours an insertion of a lentiposon cassette in the *Stag3* gene that leads to a null allele (18). The STAG3 mutation was maintained on a pure Friend Virus B-type genetic background. Mice were genotyped by polymerase chain reaction from tail biopsies, using the primers 5′-TGAGGTTTTTCAGCA GTGGCATT-3′and 5′-GCTGCTGGAAAGGGAAAGTCAG.

T-3′ for the wild-type allele; 5′-CTTCAAACTCCTGCTT CAGGTT-3′ (391 bp) and 5′-TCACAAAAACAGTGTCCTC TGG-3′ and 5′-CGTCTGTTGTGTGACTCTG.

GTAAC-3′ for the targeted allele (494 bp). REC8 and RAD21L mutants have been previously described (13,16).

All animal experiments were performed in accordance with procedures approved by the institutional animal ethics committees.

### FACs analysis

*Stag3l*$^{+/+}$ and *Stag3*$^{-/-}$ testicular cells preparation and their DNA content measurement were performed by a standard procedure (30).

### OA assay

Testes were detunicated and spermatocytes were short-term cultured as previously described (15). Briefly, $5 \times 10^6$ cell/ml were plated in 35 mm culture dishes in complete medium supplemented with 25 mM (4-(2-hydroxyethyl)-1-piperazineethanesulfonic acid). Cells were cultured at 32°C for 5–6 h with 5 μM OA (Sigma-Aldrich, St Louis, MO, USA) in 7% $CO_2$. Spreading and immunofluorescence was performed following the 'dry-down' technique as previously described (42).

### Histology

Mice were perfused and their testes extracted or directly fixed in Bowin's fixative and processed into serial paraffin sections and stained with hematoxylin-eosin. For TUNEL assay, sections were deparaffinized and apoptotic cells were detected with the In Situ Cell Death Detection Kit (Roche Mannheim, Germany) and counterstained with 4',6-diamidino-2-phenylindole. Apoptotic cells were pseudocolored in green.

## SUPPLEMENTARY MATERIAL

Supplementary Material is available at *HMG* online.

## ACKNOWLEDGEMENTS

E.L., L.G.H., I.G.T. and A.M.P. thank the pathology unit of the CIC-Salamanca. We express our sincere thanks to A. Losada and T. de Lange for kindly providing antibodies and to I. Ramos-Fernández for technical assistance. We thank the two anonymous referees for providing us with constructive comments and suggestions.

*Conflict of Interest statement*. None declared.

## FUNDING

This work was supported by grant SAF2011-25252 and Junta de Castilla y León (E.L. and A.M.P.). S.C. and R.A.V. are supported by the University Paris Diderot-Paris7, the Ligue Nationale contre le Cancer, the Centre National de la Recherche Scientifique (CNRS) and the GIS-Institut des Maladies Rares.

## REFERENCES

1. Jarow, J.P., Espeland, M.A. and Lipshultz, L.I. (1989) Evaluation of the azoospermic patient. *J. Urol.*, **142**, 62–65.
2. Ferlin, A., Arredi, B. and Foresta, C. (2006) Genetic causes of male infertility. *Reprod. Toxicol.*, **22**, 133–141.
3. Jarow, J.P., Sharlip, I.D., Belker, A.M., Lipshultz, L.I., Sigman, M., Thomas, A.J., Schlegel, P.N., Howards, S.S., Nehra, A., Damewood, M.D. *et al.* (2002) Best practice policies for male infertility. *J. Urol.*, **167**, 2138–2144.
4. Bhasin, S., de Kretser, D.M. and Baker, H.W. (1994) Pathophysiology and natural history of male infertility. *J. Clin. Endocrinol. Metab.*, **79**, 1525–1529.
5. Matsumiya, K., Namiki, M., Takahara, S., Kondoh, N., Takada, S., Kiyohara, H. and Okuyama, A. (1994) Clinical study of azoospermia. *Int. J. Androl.*, **17**, 140–142.
6. Reijo, R., Alagappan, R.K., Patrizio, P. and Page, D.C. (1996) Severe oligozoospermia resulting from deletions of azoospermia factor gene on Y chromosome. *Lancet*, **11**, 1290–1293.
7. Van Assche, E., Bonduelle, M., Tournaye, H., Joris, H., Verheyen, G., Devroey, P., Van Steirteghem, A. and Liebaers, I. (1996) Cytogenetics of infertile men. *Hum. Reprod.*, **11**, 1–24; discussion 25–26.
8. Dohle, G.R., Halley, D.J., Van Hemel, J.O., van den Ouwel, A.M., Pieters, M.H., Weber, R.F. and Govaerts, L.C. (2002) Genetic risk factors in infertile men with severe oligozoospermia and azoospermia. *Hum. Reprod.*, **17**, 13–16.
9. Lu, C., Xu, M., Wang, R., Qin, Y., Wang, Y., Wu, W., Song, L., Wang, S., Shen, H., Sha, J. *et al.* (2014) Pathogenic variants screening in five non-obstructive azoospermia associated genes. *Mol. Hum. Reprod.*, **20**, 178–183.
10. Zhao, H., Xu, J., Zhang, H., Sun, J., Sun, Y., Wang, Z., Liu, J., Ding, Q., Lu, S., Shi, R. *et al.* (2012) A genome-wide association study reveals that variants within the HLA region are associated with risk for nonobstructive azoospermia. *Am. J. Hum. Genet.*, **90**, 900–906.
11. Hu, Z., Xia, Y., Guo, X., Dai, J., Li, H., Hu, H., Jiang, Y., Lu, F., Wu, Y., Yang, X. *et al.* (2011) A genome-wide association study in Chinese men identifies three risk loci for non-obstructive azoospermia. *Nat. Genet.*, **44**, 183–186.
12. Llano, E., Herrán, Y., García-Tuñón, I., Gutiérrez-Caballero, C., de Álava, E., Barbero, J.L., Schimenti, J., de Rooij, D.G., Sánchez-Martín, M. and Pendás, A.M. (2012) Meiotic cohesin complexes are essential for the formation of the axial element in mice. *J. Cell Biol.*, **197**, 877–885.
13. Herran, Y., Gutiérrez-Caballero, C., Sánchez-Martín, M., Hernández, T., Viera, A., Barbero, J.L., de Álava, E., de Rooij, D.G., Suja, J.Á., Llano, E. and Pendás, A.M. (2011) The cohesin subunit RAD21L functions in meiotic synapsis and exhibits sexual dimorphism in fertility. *EMBO J.*, **30**, 3091–3105.
14. Matzuk, M.M. and Lamb, D.L. (2008) The biology of infertility: research advances and clinical challenges. *Nat. Med.*, **14**, 1197–1213.
15. Revenkova, E., Eijpe, M., Heyting, C., Hodges, C.A., Hunt, P.A., Liebe, B., Scherthan, H. and Jessberger, R. (2004) Cohesin SMC1 beta is required for meiotic chromosome dynamics, sister chromatid cohesion and DNA recombination. *Nat. Cell Biol.*, **6**, 555–562.
16. Bannister, L.A., Reinholdt, L.G., Munroe, R.J. and Schimenti, J.C. (2004) Positional cloning and characterization of mouse mei8, a disrupted allelle of the meiotic cohesin Rec8. *Genesis*, **40**, 184–194.
17. Caburet, S., Zavadakova, P., Ben-Neriah, Z., Bouhali, K., Dipietromaria, A., Charon, C., Besse, C., Laissue, P., Chalifa-Caspi, V., Christin-Maitre, S. *et al.* (2012) Genome-wide linkage in a highly consanguineous pedigree reveals two novel loci on chromosome 7 for non-syndromic familial premature ovarian failure. *PLoS One*, **7**, e33412.
18. Caburet, S., Arboleda, V.A., Llano, E., Overbeek, P.A., Barbero, J.L., Oka, K., Harrison, W., Vaiman, D., Ben-Neriah, Z., García-Tuñón, I. *et al.* Mutant cohesin in premature ovarian failure. *NEJM*, in press.
19. Nasmyth, K. (2011) Cohesin: a catenase with separate entry and exit gates?. *Nat. Cell Biol.*, **13**, 1170–1117.
20. Remeseiro, S. and Losada, A. (2013) Cohesin, a chromatin engagement ring. *Curr. Opin. Cell Biol.*, **25**, 63–71.
21. Gruber, S., Arumugam, P., Katou, Y., Kuglitsch, D., Helmhart, W., Shirahige, K. and Nasmyth, K. (2006) Evidence that loading of cohesin onto chromosomes involves opening of its SMC hinge. *Cell*, **127**, 523–537.
22. Prieto, I., Suja, J.A., Pezzi, N., Kremer, L., Martínez-A, C., Rufas, J.S. and Barbero, J.L. (2001) Mammalian STAG3 is a cohesin specific to sister chromatid arms in meiosis I. *Nat. Cell Biol.*, **3**, 761–766.
23. Gutiérrez-Caballero, C., Herrán, Y., Sánchez-Martín, M., Suja, J.A., Barbero, J.L., Llano, E. and Pendás, A.M. (2011) Identification and molecular characterization of the mammalian α-kleisin RAD21L. *Cell Cycle*, **10**, 1477–1487.

24. Fraune, J., Schramm, S., Alsheimer, M. and Benavente, R. (2012) The mammalian synaptonemal complex: protein components, assembly and role in meiotic recombination. *Exp. Cell Res.*, **318**, 1340–1346.
25. Bolcun-Filas, E. and Schimenti, J.C. (2012) Genetics of meiosis and recombination in mice. *Int. Rev. Cell Mol. Biol.*, **298**, 179–227.
26. Yuan, L., Liu, J.-G., Zhao, J., Brundell, E., Daneholt, B. and Hoog, C. (2000) The murine SCP3 gene is required for synaptonemal complex assembly, chromosome synapsis, and male fertility. *Mol. Cell*, **5**, 73–83.
27. Yuan, L., Liu, J.-G., Hoja, M.R., Wilbertz, J., Nordqvist, K. and Hoog, C. (2002) Female germ cell aneuploidy and embryo death in mice lacking the meiosis-specific protein SCP3. *Science*, **296**, 1115–1118.
28. Russell, L.D., Ren, H.P., Sinha Hikim, I., Schulze, W. and Sinha Hikim, A.P. (1990) A comparative study in twelve mammalian species of volume densities, volumes, and numerical densities of selected testis components, emphasizing those related to the Sertoli cell. *Am. J. Anat.*, **188**, 21–30.
29. de Rooij, D.G. and de Boer, P. (2003) Specific arrests of spermatogenesis in genetically modified and mutant mice. *Cytogenet. Genome. Res.*, **103**, 267–276.
30. Lee, J. and Hirano, T. (2011) RAD21L, a novel cohesin subunit implicated in linking homologous chromosomes in mammalian meiosis. *J. Cell Biol.*, **192**, 263–276.
31. Kudo, N.R., Anger, M., Peters, A.H., Stemmann, O., Theussl, H.C., Helmhart, W., Kudo, H., Heyting, C. and Nasmyth, K. (2009) Role of cleavage by separase of the Rec8 kleisin subunit of cohesin during mammalian meiosis I. *J. Cell Sci.*, **122**, 2686–2698.
32. Tachibana-Konwalski, K., Godwin, J., van der Weyden, L., Champion, L., Kudo, N.R., Adams, D.J. and Nasmyth, K. (2010) Rec8-containing cohesin maintains bivalents without turnover during the growing phase of mouse oocytes. *Genes Dev.*, **24**, 2505–2516.
33. Biswas, U., Wetzker, C., Lange, J., Christodoulou, E.G., Seifert, S., Beyer, A. and Jessberguer, R. (2013) Meiotic cohesin SMC1B provides prophase I centromeric cohesion and is required for multiple synapsis-associated functions. *PLOS Genet.*, **9**, e1003985.
34. Redon, C., Pilch, D., Rogakou, E., Sedelnikova, O., Newrock, K. and Bonner, W. (2003) Histone H2A variants H2AX and H2AZ. *Curr. Opin. Genet. Dev.*, **12**, 162–169.
35. Mahadevaiah, S.K., Turner, J.M., Baudat, F., Rogakou, E.P., de Boer, P., Blanco-Rodríguez, J., Jasin, M., Keeney, S., Bonner, W.M. and Burgoyne, P.S. (2001) Recombinational DNA double-strand breaks in mice precede synapsis. *Nat. Genet.*, **27**, 271–276.
36. Symington, J. and Gautier, L.S. (2011) Double-strand break end resection and repair pathway choice. *Annu. Rev. Genet.*, **45**, 247–271.
37. Tarsounas, M., Morita, T., Pearlman, R.E. and Moens, P.B. (1999) RAD51 and DMC1 form mixed complexes associated with mouse meiotic chromosome cores and synaptonemal complexes. *J. Cell Biol.*, **147**, 207–220.
38. Scherthan, H., Jerratsch, M., Li, B., Smith, S., Hultén, M., Lock, T. and de Lange, T. (2000) Mammalian meiotic telomeres: protein composition and redistribution in relation to nuclear pores. *Mol. Biol. Cell*, **12**, 4189–4203.
39. Zickler, D. and Kleckner, N. (1999) Meiotic chromosomes: integrating structure and function. *Annu. Rev. Genet.*, **33**, 603–754.
40. Wiltshire, T., Park, C., Caldwell, K.A. and Handel, M.A. (1995) Induced premature G2/M-phase transition in pachytene spermatocytes includes events unique to meiosis. *Dev. Biol.*, **169**, 557–567.
41. Ishiguro, K., Kim, J., Fujiyama-Nakamura, S., Kato, S. and Watanabe, Y. (2011) A new meiosis-specific cohesin complex implicated in the cohesin code for homologous pairing. *EMBO Rep.*, **12**, 267–275.
42. Xu, H., Beasley, M.D., Warren, W.D., van der Horst, G.T. and McKay, M.J. (2005) Absence of mouse REC8 cohesin promotes synapsis of sister chromatids in meiosis. *Dev. Cell*, **8**, 949–961.
43. Bannister, L.A., Pezza, R.J., Donaldson, J.R., de Rooij, D.G., Schimenti, K.J., Camerini-Otero, R.D. and Schimenti, J.C. (2007) A dominant, recombination-defective allele of Dmc1 causing male-specific sterility. *PLoS Biol.*, **5**. e105.
44. Hikiba, J., Takizawa, Y., Ikawa, S., Shibata, T. and Kurumizaka, H. (2009) Biochemical analysis of the human DMC1-I37N polymorphism. *FEBS J.*, **276**, 457–465.
45. Peters, A.H., Plug, A.W., van Vugt, M.J. and de Boer, P. (1997) A drying-down technique for the spreading of mammalian meiocytes from the male and female germline. *Chromosome Res.*, **5**, 66–68.
46. Prieto, I., Tease, C., Pezzi, N., Buesa, J.M., Ortega, S., Kremer, L., Martínez, A.C., Hultén, M.A. and Barbero, J.L. (2004) Cohesin component dynamics during meiotic prophase I in mammalian oocytes. *Chromosome Res.*, **12**, 197–213.